Efficient Characterization of Repolarization Adaptation to Heart Rate Changes

A Mincholé[1,2], E Zacur[2], E Pueyo[1,2], P Laguna[2,1]

[1]Centro de Investigación Biomédica en Red, CIBER-BBN, Spain;
[2]I3A, University of Zaragoza, Spain;

Abstract

This work aims at providing a efficient method to estimate the parameters of a non linear model with memory previously proposed to characterize rate adaptation of repolarization indices. The physiological restrictions on the model parameters have been included in the cost function in such a way that unconstrained optimization techniques can be used for parameter estimation. The proposed method has been evaluated on ECG recordings of healthy subjects performing a tilt test, where rate adaptation of QT and T_{peak}-to-T_{end} (T_{pe}) intervals has been characterized. Results show that the T_{pe} interval adapts faster to changes in heart rate than the QT interval.

Keywords *Rate adaptation, T peak to T end interval, QT interval*

1 Introduction

QT and T_{peak}-to-T_{end} (T_{pe}) intervals are commonly used to describe overall repolarization duration and its spatial dispersion [1]. Changes in these intervals have been related to increased arrhythmic risk under a variety of clinical conditions [1].

The QT interval is known to be influenced by changes in heart rate (HR) and the use of HR correction is crucial in the estimation of QT prolongation. However, the rate dependence of the T_{pe} interval is still an issue. Previous studies characterizing T_{pe} rate dependence are controversial, with T_{pe} shown to be independent of HR by some authors [2] and markedly HR dependent by others [3].

In this work, a model previously proposed to estimate QT rate adaptation [4] was used to estimate both, QT and T_{pe} rate adaptation. The physiological restrictions on the model parameters and the computational time required for the estimation led us to propose a efficient estimation method that uses a QuasiNewton optimization technique. This technique was used in [5] and details are given in this manuscript.

The proposed method was evaluated in ECG recordings presenting HR changes, in which T_{pe} rate adaptation was characterized and compared to QT rate adaptation.

2 Methods

2.1 Model formulation

The input $x_{\text{RR}}[n]$ and output $y_{\text{T}_{pe}}[n]$ denote the RR and the T_{pe} series of each recording sampled to $f_s = 1$ Hz. The problem consists of identifying two blocks, a FIR filter and a nonlinear function, which relate $x_{\text{RR}}[n]$ and $y_{\text{T}_{pe}}[n]$, as shown in Fig.1 (analogously for the QT interval).

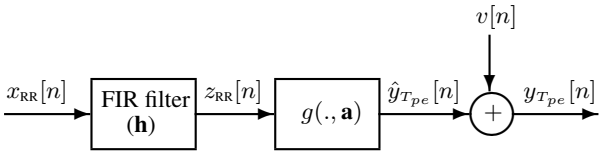

Figure 1: Block diagram describing the relationship between RR and T_{pe} consisting of a time invariant FIR filter with impulse response **h**, and a nonlinear function parameterized by vector **a**.

The first block corresponds to a time invariant Nth-order FIR filter with impulse response:

$$\mathbf{h} = (h[1],\ \ldots\ , h[N])^T \tag{1}$$

whose output is denoted by $z_{\text{RR}}[n]$. Impulse response $\mathbf{h}$ includes information about the memory of the system, that is, a characterization of the influence of a history of previous RR intervals on each T_{pe} (analogously for QT) measurement.

The order N of filter $\mathbf{h}$ was set to 150 samples corresponding to 150 seconds, expected to exceed the T_{pe} and QT memory lag for the population used in this study.

The second block is a function $g_k(.,\mathbf{a})$, which is parameterized with the biparameter vector $\mathbf{a} = [a_0,\ a_1]^T$. $g_k(.,\mathbf{a})$ represents the relationship between the RR interval and the T_{pe} or QT interval once the memory effect has been compensated for, and it was particularized and optimized for each subject using one of the regression functions described below, denoted g_k.

The output of the model $\hat{y}_{\text{T}_{pe}}[n]$ is defined as:

$$\hat{y}_{\text{T}_{pe}}[n] = g_k(z_{\text{RR}}[n], \mathbf{a}) \tag{2}$$

In vector notation, $\mathbf{z}_{\text{RR}}$, is the convolution between the input vector $\mathbf{x}_{\text{RR}}$ and the impulse response $\mathbf{h}$, and can be

expressed as $\mathbf{z}_{\text{RR}} = \mathbf{x}_{\text{RR}} * \mathbf{h} = \mathbf{X}_{\text{RR}}\mathbf{h}$, where $\mathbf{X}_{\text{RR}}$ is the Toeplitz matrix of $\mathbf{x}_{\text{RR}}$:

$$\mathbf{X}_{\text{RR}} = \begin{bmatrix} x_{\text{RR}}[N] & x_{\text{RR}}[N-1] & \dots & x_{\text{RR}}[1] \\ x_{\text{RR}}[N+1] & x_{\text{RR}}[N] & & \\ \vdots & \vdots & \ddots & \vdots \\ x_{\text{RR}}[M] & x_{\text{RR}}[M-1] & \dots & x_{\text{RR}}[M-N+1] \end{bmatrix} \tag{3}$$

which is a $(M - N + 1) \times N$ matrix, where M is the length of the signal $x_{\text{RR}}[n]$.

Different biparametric regression functions that span from a linear to a hyperbolic relationship, as described in [4], were considered for $g_k(., \mathbf{a})$, and the one that best fits the data of each subject is identified. Two examples are:

$$\text{Linear: } y_{T_{pe}}[n] = g_1(z_{\text{RR}}[n], \mathbf{a}) = a_0 + a_1 z_{\text{RR}}[n] \tag{4}$$

$$\text{Hyperbolic: } y_{T_{pe}}[n] = g_2(z_{\text{RR}}[n], \mathbf{a}) = a_0 + \frac{a_1}{z_{\text{RR}}[n]} \tag{5}$$

The optimum values of the FIR filter response $\mathbf{h}$, vector $\mathbf{a}$, and function g_k were searched for by minimizing a least square estimator between the estimated output $\hat{y}_{T_{pe}}[n]$ (see eq.(2)) and the T_{pe} interval series $y_{T_{pe}}[n]$, for each subject independently using its whole recording.

$$J_k^{LS}(\mathbf{h}, \mathbf{a}) = \left\| \mathbf{y}_{T_{pe}} - g_k(\mathbf{x}_{\text{RR}} * \mathbf{h}, \mathbf{a}) \right\|^2 \tag{6}$$

However, as described in [4], this optimization problem is an 'ill-posed' problem which can have multiple solutions. When dealing with 'ill-posed' problems, a regularization term including a priori information of the solution, should be added. This study uses a Tikhonov regularization approach [6].

Rate dependence of repolarization features have been modelled as exponential decays, so penalizing the deviations of $\mathbf{h}$ from having an exponential decay is used to construct the regularization matrix $\mathbf{D}$ as in [4].

$$\mathbf{D} = \begin{bmatrix} \tau & -1 & 0 & \dots & 0 \\ 0 & \tau & -1 & \ddots & \\ \vdots & & \ddots & \ddots & \\ 0 & \dots & 0 & \tau & -1 \end{bmatrix} \tag{7}$$

Note that in case of $\mathbf{h}$ having an exponential decay expressed as $h[j] = e^{-\lambda j} = \tau^j$, the equality $\|\mathbf{Dh}\| = 0$ holds.

The value of τ is calculated as the best exponential decay of $\mathbf{h}$ that leads to the minimum mean square error between $\mathbf{y}_{T_{pe}}$ and $\hat{\mathbf{y}}_{T_{pe}}$ using the linear regression model g_1.

The estimator thus turns into a regularized least square estimator:

$$\{\mathbf{h}^*, \mathbf{a}^*, k^*\} = \arg \min_{\{\mathbf{h}, \mathbf{a}, k\}} \left(J_k^{LS}(\mathbf{h}, \mathbf{a}) + \beta^2 \|\mathbf{Dh}\|^2 \right) \tag{8}$$

where β^2 is a regularization parameter that control how much weight is given to the energy of $\|\mathbf{Dh}\|$ relative to the energy of the residual $\left\| \mathbf{y}_{T_{pe}} - \hat{\mathbf{y}}_{T_{pe}} \right\|$. The value of β was obtained by using the "L-curve" criterion [7].

Regarding k^* in eq.(8), the optimum regression function $g_k(., \mathbf{a})$ was determined as the one that minimizes the mean square error for each subject independently.

Then, the cost function to be minimized for each regression function is:

$$J_k(\mathbf{h}, \mathbf{a}) = \left\| \mathbf{y}_{T_{pe}} - g_k(\mathbf{x}_{\text{RR}} * \mathbf{h}, \mathbf{a}) \right\|^2 + \beta^2 \|\mathbf{Dh}\|^2 \tag{9}$$

where the first term corresponds to the residual energy of the model and the second one corresponds to the regularization energy.

Restrictions: The optimal estimation of $\mathbf{h}$ is subject to two constraints: the sum of the $\mathbf{h}$ components has to be 1 ($\sum_{i=1}^{N} h[i] = 1$), to ensure normalized filter gain, and all the components of $\mathbf{h}$ have to be non-negative ($h[i] \geq 0$), to give a physiological plausible interpretation.

2.2 Optimization including restrictions

In this work we reformulated $\mathbf{h}$ in order to incorporate both constraints into the cost function, and we used a "Quasi-Newton" optimization technique to minimize the new cost function.

In order to minimize the cost function in eq.(9), subject to the previously described constraints, we propose to define $h[i] = \frac{\tilde{h}^2[i]}{\sum \tilde{h}^2[i]}$, and optimize over $\tilde{\mathbf{h}}$ without any constraints.

Then, we obtain a new function to optimize:

$$\tilde{J}_k(\tilde{\mathbf{h}}, \mathbf{a}) = J_k\left(\frac{\tilde{\mathbf{h}}^2}{\sum \tilde{h}[i]^2}, \mathbf{a} \right) \quad \text{with } h[i] = \frac{\tilde{h}^2[i]}{\sum \tilde{h}^2[i]} \tag{10}$$

over which, unconstrained optimization techniques can be used. $\tilde{\mathbf{h}}^2$ is defined as $\tilde{\mathbf{h}}^2 = \left[\tilde{h}^2[1], \tilde{h}^2[2], \dots, \tilde{h}^2[N] \right]$.

The new cost function $\tilde{J}_k(\tilde{\mathbf{h}}, \mathbf{a})$ is optimized over $\tilde{\mathbf{h}}$ and over $\mathbf{a}$ for each regression function g_k. The estimated $\hat{\mathbf{y}}_{T_{pe}}$ depends on the regression function $g_k(\mathbf{z}_{\text{RR}}, \mathbf{a})$, which depends on $\mathbf{h}$ by the relationship $\mathbf{z}_{\text{RR}} = \mathbf{x}_{\text{RR}} * \mathbf{h}$. Then, in order to differentiate the cost function $\tilde{J}_k$ with respect to the first variable vector $\tilde{\mathbf{h}}$, the chain rule is applied:

$$\frac{\partial \tilde{J}}{\partial \tilde{\mathbf{h}}} = \frac{\partial \tilde{J}}{\partial g_k(., \mathbf{a})} \cdot \frac{\partial g_k(., \mathbf{a})}{\partial \mathbf{h}} \cdot \frac{\partial \mathbf{h}}{\partial \tilde{\mathbf{h}}} + \beta^2 \frac{\partial \|\mathbf{Dh}\|^2}{\partial \mathbf{h}} \cdot \frac{\partial \mathbf{h}}{\partial \tilde{\mathbf{h}}} \tag{11}$$

where the first term represents the estimation error and the second one the regularization term.

- The derivative $\frac{\partial \mathbf{h}}{\partial \tilde{\mathbf{h}}}$, also called Jacobian matrix, is defined as the matrix of the derivatives of a vector-valued function with respect to another vector. It represent the effect on $\mathbf{h}$ of a perturbation, $\mathrm{d}\tilde{\mathbf{h}}$, of the vector $\tilde{\mathbf{h}}$:

$$\begin{pmatrix} \mathrm{d}h[1] \\ \vdots \\ \mathrm{d}h[N] \end{pmatrix} = \begin{bmatrix} \frac{\mathrm{d}h[1]}{\mathrm{d}\tilde{h}[1]} & \dots & \frac{\mathrm{d}h[1]}{\mathrm{d}\tilde{h}[N]} \\ \vdots & \ddots & \vdots \\ \frac{\mathrm{d}h[N]}{\mathrm{d}\tilde{h}[1]} & \dots & \frac{\mathrm{d}h[N]}{\mathrm{d}\tilde{h}[N]} \end{bmatrix} \begin{pmatrix} \mathrm{d}\tilde{h}[1] \\ \vdots \\ \mathrm{d}\tilde{h}[N] \end{pmatrix}$$

Therefore, the derivative:

$$\frac{\partial \mathbf{h}}{\partial \tilde{\mathbf{h}}} = \begin{bmatrix} \frac{\mathrm{d}h[1]}{\mathrm{d}\tilde{h}[1]} & \cdots & \frac{\mathrm{d}h[1]}{\mathrm{d}\tilde{h}[N]} \\ \vdots & \ddots & \vdots \\ \frac{\mathrm{d}h[N]}{\mathrm{d}\tilde{h}[1]} & \cdots & \frac{\mathrm{d}h[N]}{\mathrm{d}\tilde{h}[N]} \end{bmatrix} =$$

$$= \begin{bmatrix} \frac{2\tilde{h}[1]\sum \tilde{h}[i]^2 - 2\tilde{h}[1]^3}{(\sum \tilde{h}[i]^2)^2} & \cdots & \frac{-2\tilde{h}[N]\tilde{h}[1]^2}{(\sum \tilde{h}[i]^2)^2} \\ \vdots & \ddots & \vdots \\ \frac{-2\tilde{h}[1]\tilde{h}[N]^2}{(\sum \tilde{h}[i]^2)^2} & \cdots & \frac{2\tilde{h}[N]\sum \tilde{h}[i]^2 - 2\tilde{h}[N]^3}{(\sum \tilde{h}[i]^2)^2} \end{bmatrix} \quad (12)$$

- Calculation of $\frac{\partial \tilde{J}_k}{\partial g_k(.,\mathbf{a})}$:

$$\tilde{J}_k = \left\| \mathbf{y}_{T_{pe}} - g_k(\mathbf{z}_{\text{RR}}, \mathbf{a}) \right\|^2 + \beta^2 \left\| \mathbf{Dh} \right\|^2$$
$$= \left(\mathbf{y}_{T_{pe}} - g_k(\mathbf{z}_{\text{RR}}, \mathbf{a})\right)^T \left(\mathbf{y}_{T_{pe}} - g_k(\mathbf{z}_{\text{RR}}, \mathbf{a})\right) + \beta^2 \left\| \mathbf{Dh} \right\|^2$$

Therefore [1],

$$\frac{\partial \tilde{J}_k}{\partial g_k(., \mathbf{a})} = -2 \cdot \left(\mathbf{y}_{T_{pe}} - g_k(\mathbf{z}_{\text{RR}}, \mathbf{a})\right)^T \quad (13)$$

- Calculation of $\frac{\partial g_k(.,\mathbf{a})}{\partial \mathbf{h}}$:

Taking into account that g_k depends on $\mathbf{z}_{\text{RR}}$, and $\mathbf{z}_{\text{RR}} = \mathbf{X}_{\text{RR}}\mathbf{h}$:

$$\frac{\partial g_k(\mathbf{z}_{\text{RR}}, \mathbf{a})}{\partial \mathbf{h}} = \frac{\partial g_k(\mathbf{z}_{\text{RR}}, \mathbf{a})}{\partial \mathbf{z}_{\text{RR}}} \cdot \frac{\partial \mathbf{z}_{\text{RR}}}{\partial \mathbf{h}} = \frac{\partial g_k(\mathbf{z}_{\text{RR}}, \mathbf{a})}{\partial \mathbf{z}_{\text{RR}}} \cdot \mathbf{X}_{\text{RR}} \quad (14)$$

$\frac{\partial g_k(\mathbf{z}_{\text{RR}}, \mathbf{a})}{\partial \mathbf{z}_{\text{RR}}}$ is a matrix since $\partial g_k(\mathbf{z}_{\text{RR}}, \mathbf{a})$ and $\partial \mathbf{z}_{\text{RR}}$ are vectors. Besides, a perturbation of the i^{th} element of the vector $\mathbf{z}_{\text{RR}}$, produces an effect only on the i^{th} element of the vector $g_k(\mathbf{z}_{\text{RR}}, \mathbf{a})$, and then $\frac{\partial g_k(\mathbf{z}_{\text{RR}}, \mathbf{a})}{\partial \mathbf{z}_{\text{RR}}}$ is a diagonal matrix.

For the two regression model examples shown in equations (4) and (5) , the diagonal of $\frac{\partial g_k(\mathbf{z}_{\text{RR}}, \mathbf{a})}{\partial \mathbf{z}_{\text{RR}}}$ are shown in Table 1.

MODEL (g_k)	$\text{diag}\left(\frac{\partial g_k(.,\mathbf{a})}{\partial \mathbf{z}_{\text{RR}}}\right)$	$\frac{\partial g_k(.,\mathbf{a})}{\partial a_0}$	$\frac{\partial g_k(.,\mathbf{a})}{\partial a_1}$
$a_0 + a_1 \mathbf{z}_{\text{RR}}$	$a_1\,\mathbf{1}$	$\mathbf{1}$	$\mathbf{z}_{\text{RR}}$
$a_0 + \frac{a_1}{\mathbf{z}_{\text{RR}}}$	$-\frac{a_1}{\mathbf{z}_{\text{RR}}^2}$	$\mathbf{1}$	$\frac{1}{\mathbf{z}_{\text{RR}}}$

Table 1: Example of the derivatives of two regression functions $g_k(\mathbf{z}_{\text{RR}}, \mathbf{a})$, with respect to $\mathbf{z}_{\text{RR}}$ and $\mathbf{a}$. $\text{diag}\left(\frac{\partial g_k(.,\mathbf{a})}{\partial \mathbf{z}_{\text{RR}}}\right)$ is the diagonal of the matrix $\frac{\partial g_k(.,\mathbf{a})}{\partial \mathbf{z}_{\text{RR}}}$. $\mathbf{1}$ represents a N-length vector of ones. All mathematical expressions are element-wise.

- The derivative $\frac{\partial \|\mathbf{Dh}\|^2}{\partial \mathbf{h}}$:

$$\frac{\partial \left\| \mathbf{Dh} \right\|^2}{\partial \mathbf{h}} = \frac{\partial}{\partial \mathbf{h}} (\mathbf{Dh})^T (\mathbf{Dh}) = 2(\mathbf{Dh})^T \mathbf{D} \quad (15)$$

[1] $d(Ax+b)^T(Ax+b) = 2(Ax+b)^T A\, dx$, where A is a matrix and x and b are vectors.

Eventually, $\frac{\partial \tilde{J}_k}{\partial \tilde{\mathbf{h}}}$ can be computed by introducing equations (12), (13), (14) and (15) into (11).

In order to differentiate the cost function $\tilde{J}_k$ with respect to the second variable vector $\mathbf{a} = [a_0, a_1]^T$, the chain rule is also applied:

$$\frac{\partial \tilde{J}_k}{\partial \mathbf{a}} = \frac{\partial \tilde{J}_k}{\partial g_k(., \mathbf{a})} \cdot \frac{\partial g_k(., \mathbf{a})}{\partial \mathbf{a}} \quad (16)$$

The first term is already calculated in eq.(13), while the second term is a Nx2 matrix where the first column corresponds to $\frac{\partial g_k(.,\mathbf{a})}{\partial a_0}$ and the second column to $\frac{\partial g(.,\mathbf{a})}{\partial a_1}$, both shown in Table 1.

2.2.1 Optimization technique

In this work, a *Quasi-Newton* optimization technique, the BFGS (Broyden-Fletcher-Goldfarb-Shanno), is used to minimize the cost function $\tilde{J}_k(\tilde{\mathbf{h}}, \mathbf{a})$ [8].

BFGS *Quasi-Newton* method estimate the Hessian (or the Hessian inverse) matrix preserving symmetry and positive definiteness. In each step, the estimation of the Hessian matrix is updated using the gradient information [8].

In order to compute the step size along the descent direction, obtained by the Quasi-Newton method, a *parabolic* and a *golden ratio* line searches were used [9].

2.3 Population

Fifteen ECG recordings obtained during a the head-up tilt test trial, sampled at a frequency of 1000 Hz, were used to characterize T_{pe} and QT rate adaptation. The tilt test protocol generated two step-like RR changes with stabilized RR intervals after each of them (see Fig.2, top panel).

ECG delineation was performed using a wavelet-based delineator [10]. RR, QT and T_{pe} intervals were computed from the ECG delineation marks in the V2 and V4 leads.

2.4 Quantification of the results

The time required for T_{pe} and QT to complete 90% of their rate adaptation, denoted by t_{90}, was computed by setting a threshold of 0.1 to the cumulative sum of the filter impulse response, $c[n]$:

$$c[n] = \sum_{i=n}^{N} h[i], \quad \text{leading to}$$

$$t_{90} = \frac{1}{f_s} \arg\max_n \left(c[n] > 0.1\right) \quad (17)$$

The cumulative sum $c[n]$, represents the response of a step function to the FIR filter $h[n]$.

3 Results and Discussion

An example of the reconstruction of the $y_{\text{QT}}[n]$ and $y_{T_{pe}}[n]$ series, after estimating the corresponding $h[n]$, the regression model k and its coefficient vector $\mathbf{a}$ are

shown in Fig.2. The reconstructions $\hat{y}_{\mathrm{T}_{pe}}[n]$ and $\hat{y}_{\mathrm{QT}}[n]$, shown in black solid lines, begin after 150 seconds corresponding to the length of the filter $h[n]$. The estimated regression functions in this example are different for the QT (linear model) and for the T_{pe} series (parabolic model).

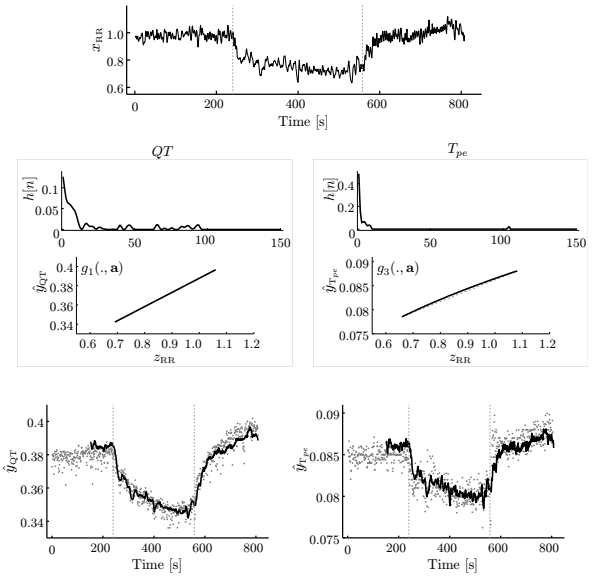

Figure 2: Top panel: x_{RR} series obtained from a subject of the study population. Middle and bottom panels: on the left, an example of how the reconstruction $\hat{y}_{\mathrm{QT}}$ (in black solid line) of the QT interval series y_{QT} (in gray dots), is obtained by x_{RR} through the estimations of $h[n]$ and $g_k(.,\mathbf{a})$. In this example, the optimum regression model for the QT interval is the linear one (k=1). On the right, analogously for the T_{pe}, the reconstruction $\hat{y}_{\mathrm{T}_{pe}}$ (in black solid line) is shown. The optimum model regression in this case is the parabolic function (k=3). In dashed gray line, the linear function is also depicted for comparison purposes.

In Fig.3, the median, first and third quartile of the T_{pe} rate adaptation, $c[n]$, across the 15 recordings are shown and compared to those of the QT interval. t_{90} values are 23 seconds, in mean, for T_{pe} to complete 90% of the rate adaptation and 74 seconds for QT. The characterization of T_{pe} rate adaptation, shows that T_{pe} is rate related and it has a shorter memory lag than the QT interval.

4 Conclusions

In this work a efficient estimation of the parameters of a model aimed at characterizing rate adaptation of repolarization features has been proposed. The physiological restrictions have been included into the cost function, which allowed the use of descent optimization methods with a faster convergence. The evaluation of the method on a tilt test database shows results within clinical ranges.

Acknowledgements

This work was supported in part by the Ministerio de Ciencia y Tecnología, Spain, under Project TEC2010-19410 and Project TEC2010-21703-C03-02, in part by the Diputación General de Aragón (DGA), Spain, under Grupos Consolidados GTC ref:T30, PI165/09, and PI 144/2009, in part by the ISCIII, Spain, and through CIBER-BBN CB06/01/0062.

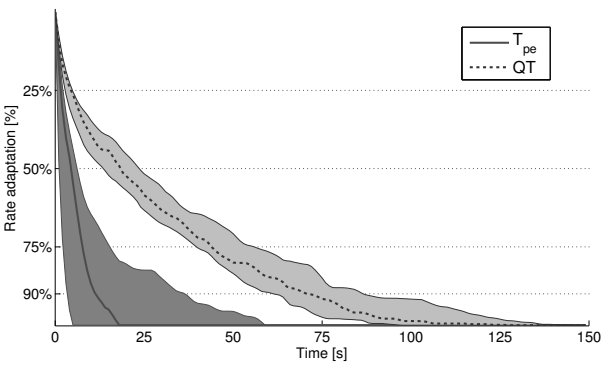

Figure 3: Median, first and third quartile of the rate adaptation, $c[n]$, of T_{pe} and QT intervals.

References

[1] C. Antzelevitch, S. Viskin, W. Shimizu, G-X Yan, P. Kowey, L. Zhang, S. Sicouri, J.M. Di Diego, and A. Burashnikov. Does Tpeak-Tend provide an index of transmural dispersion of repolarization? *Heart Rhythm*, 4(8):1114–1119, 2007.

[2] M. P. Andersen, J. Q. Xue, C. Graff, J. K. Kanters, E. Toft, and J. J. Struijk. New descriptors of T-wave morphology are independent of heart rate. *Journal of Electrocardiology*, 41(6):557–561, 2008.

[3] P. Smetana, V. Batchvarov, K Hnatkova, A. J. Camm, and M. Malik. Sex differences in the rate dependence of the t wave descending limb. *Cardiovasc Res*, 58(3):549–554, 2003.

[4] E. Pueyo, P. Smetana, P. Caminal, Bayes, M. Malik, and P. Laguna. Characterization of QT interval adaptation to RR interval changes and its use as a risk-stratifier of arrhythmic mortality in amiodarone-treated survivors of acute myocardial infarction. *IEEE Trans. Biomed. Eng.*, 51(9):1511–1520, 2004.

[5] A. Mincholé, E. Pueyo, J.F. Rodríguez, E. Zacur, M. Doblaré, and P. Laguna. Quantification of restitution dispersion from the dynamic changes of the t wave peak to end, measured at the surface ecg. *IEEE Trans. Biomed. Eng.*, 58(5):1172–1182, 2011.

[6] P. C. Hansen. *Rank-deficient and Discrete ill-posed problems*. 1998.

[7] P. C. Hansen. Analysis of discerte ill-posed problems by means of the L-curve. *SIAM Review*, 34(4):561–580, 1992.

[8] J. Nocedal and S. J. Wright. *Numerical Optimization*, chapter 6, pages 135–143. Springer, 2000.

[9] W.H. Press, S.A. Teukolsky, W.T. Vetterling, and B.P. Flannery. *Numerical Recipes: The Art of Scientific Computing*. Cambridge University Press, 2007.

[10] J.P. Martínez, R. Almeida, S. Olmos, A.P. Rocha, and P. Laguna. A Wavelet-Based ECG Delineator: Evaluation on Standard Databases. *IEEE Trans. Biomed. Eng.*, 51(4):570–581, 2004.